III.3

Pulmonary Embolism Imaging with MDCT

Joseph J. Kavanagh, Douglas R. Lake and Philip Costello

Introduction

The timely and accurate diagnosis of acute pulmonary embolism (PE) is crucial to providing appropriate patient care. Acute PE is a treatable condition with a 3-month mortality rate greater than 15% [1]. Potential complications include cardiogenic shock, hypotension, and myocardial infarction. PE is a relatively common condition, with an estimated overall incidence of about 1 per 1,000 patients within the United States [2]. Of approximately 1,000 computed tomography (CT) studies recently performed to assess for PE at our institution, roughly 10% were found to have PE. Unfortunately, the presenting symptoms of acute PE are relatively nonspecific and may be challenging for the clinician. Symptoms include dyspnea, cough, chest pain, and infrequently, hemoptysis. Chest radiography, electrocardiography (ECG), arterial blood gas measurements, and D-dimer assays all have the potential to suggest PE, but they are nonspecific [3–9]. Radiological imaging plays a crucial role in definitive diagnosis. Many modalities, including pulmonary angiography, ventilation-perfusion scintigraphy (V/Q), compression Doppler sonography, and CT have played important roles in the diagnosis of acute PE.

Over the last 5 years, multidetector CT (MDCT) pulmonary angiography has become the initial diagnostic test of choice in many institutions. Meanwhile, conventional angiography, V/Q scan, and Doppler sonography have been relegated to adjunctive roles [10–12]. Many retrospective and some prospective studies have been completed to prove the accuracy of MDCT for detecting and excluding patients suspected of acute PE. Through this research, there has been a transition from the "gold standard" of pulmonary angiography and V/Q scintigraphy to MDCT as the modality of choice for excluding PE.

Advantages of MDCT

CT has many advantages when compared with other available modalities in the detection of PE. MDCT pulmonary angiography is a rapid test, which can be obtained in a single 10-s breath hold with a 16-slice CT system. CT also has the ability to readily detect other abnormalities that may be contributing to the patient's clinical presentation, including congestive heart failure, pneumonia, interstitial lung disease, aortic dissection, malignancy (Fig. 1), and pleural disease [13, 14].

Due to the relative frequency of PE, its high mortality rate if not treated, and our ability to adequately treat it, the diagnosis of acute PE using CT has been the subject of much research. Multiple studies comparing MDCT with selective pulmonary angiography have shown a negative pre-

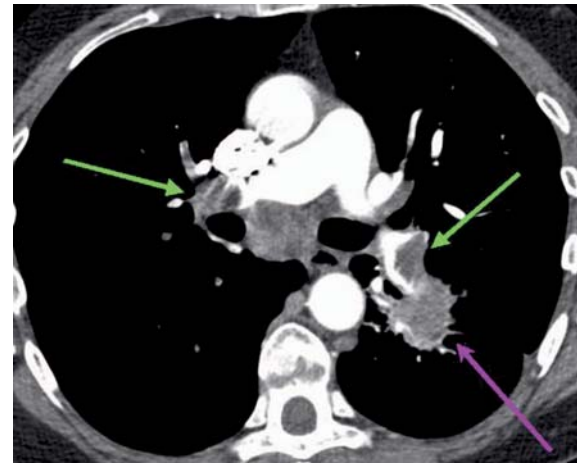

Fig. 1. A 53-year-old woman presented to the emergency department with acute shortness of breath and left-lower-extremity swelling. Multidetector computed tomography (MDCT) pulmonary angiogram axial image demonstrated large pulmonary emboli (*green arrows*) within the left and right main pulmonary arteries as well as an incidentally found left perihilar lung cancer *(purple arrow)*

Fig. 2. A computed tomography venography (CTV) exam was performed simultaneously with a CT pulmonary angiogram in a 68-year-old woman with a history of ovarian cancer presenting with dyspnea. Axial CTV image demonstrates a filling defect (*arrow*) within the right common iliac artery consistent with thrombus. Images through the chest failed to demonstrate pulmonary embolism

dictive value greater than 96% for both single-slice [15–21] and MDCT [22, 14, 23–27] in PE detection. A large prospective study by Perrier et al. [28] showed that patients with a negative D-dimer and a negative MDCT pulmonary angiogram had test less than a 1% chance of having a lower-extremity deep venous thrombosis and a 3-month follow-up thromboembolic risk of only about 1.5%. A meta-analysis of 3,500 patients with a negative CT study who did not receive anticoagulation showed a negative predictive value (NPV) of 99%, which compares favorably with NPVs of conventional pulmonary angiography and greatly exceeds that of V/Q scintigraphy (76–88%) [15, 29–32]. These studies suggest that a negative MDCT pulmonary angiogram does not require any additional radiologic tests to help exclude the presence of acute PE. Because of its high sensitivity and specificity, MDCT can be both a screening and confirmatory study. Use of CT would help decrease additional and unnecessary imaging tests and limit the time between clinical presentation and effective treatment. More recently, the greater spatial resolution of MDCT has permitted the detection of small subsegmental emboli in sixth- and seventh-order arterial branches with a high degree of interobserver agreement [33–35]. Selective pulmonary angiography has low interobserver agreement rates, ranging from 45–66% [36, 37]. Similarly, V/Q scintigraphy has not only poor interobserver agreement rates but also poor specificity of low probability studies (10%). Additionally, up to 73% of V/Q scans are reported as intermediate probability [15, 30].

In addition to imaging the pulmonary arterial system, CT venography (CTV) may be performed to assess for venous thrombosis within the pelvis and lower extremities. Delayed venous-phase images from the pelvis through the knees are obtained 180 s following intravenous contrast injection. CTV is able to detect venous thrombosis in the pelvis veins, which is typically not possible during Doppler sonography due to overlying bowel gas (Fig. 2). Acute deep venous thrombosis (DVT) on CTV is detected as a filling defect within the vein (Fig. 3). Other signs include perivenous stranding, mural enhancement, and vein enlargement [38]. A study by Cosmic et al. [39] showed that up to 11% of patients with a negative chest CT

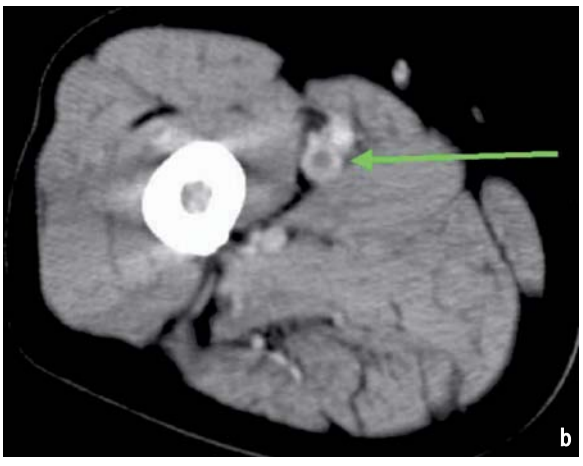

Fig. 3a, b. Axial computed tomography venography (CTV) images in two different patients presenting for CT pulmonary angiography demonstrate filling defects surrounded by intravenous contrast consistent with deep venous thrombosis (DVT) (*arrows*) in both the left common femoral vein (**a**) and right superficial femoral vein (**b**)

demonstrated venous thrombosis on CTV. Although this study did not take into account D-dimer levels, it proved the efficacy of imaging both the pelvis and lower-extremity venous structures following CT of the pulmonary arteries.

PE Findings Using MDCT

Most commonly, PE presents on CT as a filling defect within a pulmonary artery surrounded by a thin rim of contrast. These emboli often lodge at bifurcation points, extending into peripheral arteries (Fig. 4). When viewed in the transverse plane, the emboli may be described as having a "polomint" or "lifesaver" appearance (Fig. 5). When seen longitudinally, these filling defects may present as a "railway-track" sign, with the clot surrounded by contrast material within the vessel lumen (Fig. 6). Occasionally, an abrupt arterial cutoff may be encountered, with complete obstruction of the pulmonary artery [40–43].

Secondary signs of acute PE are often present and may clue the radiologist to the presence of an embolus. On lung windows, small, wedge-shaped and peripheral areas of consolidation or ground glass opacity are seen in approximately 25% of patients [44]. These opacities mostly represent areas of pulmonary hemorrhage that clear within 4–7 days, but some represent pulmonary infarcts (Fig. 7). Pulmonary infarcts on CT appear as wedge-shaped peripheral opacities often characterized as a "Hampton hump" (Fig. 8). With larger emboli, there may be regions of localized oligemia and redistribution of blood flow (mosaic perfusion) in the involved portions of lung (Fig. 9). Frequent but nonspecific signs of PE include subsegmental atelectasis and small pleural effusions.

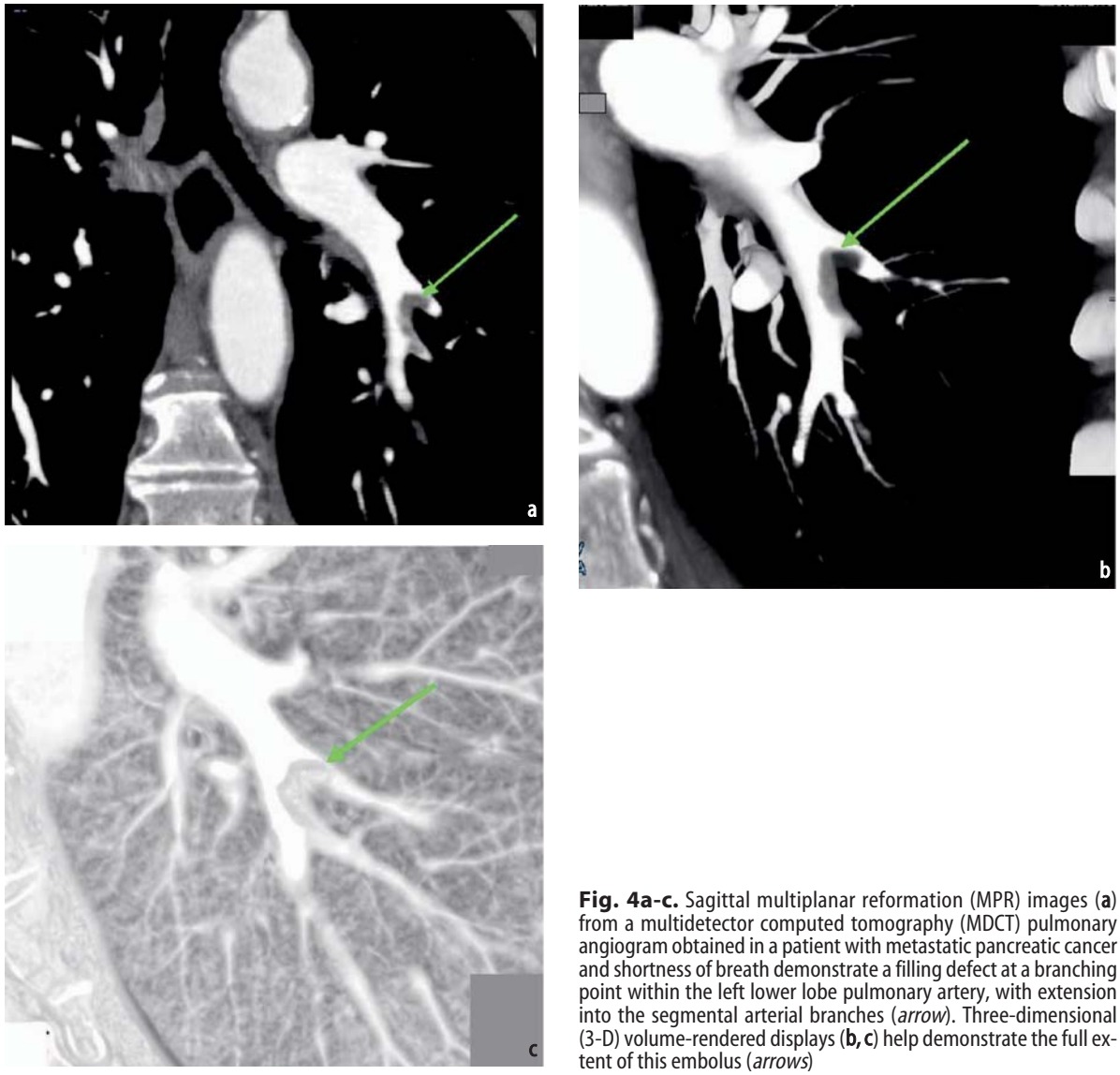

Fig. 4a-c. Sagittal multiplanar reformation (MPR) images (**a**) from a multidetector computed tomography (MDCT) pulmonary angiogram obtained in a patient with metastatic pancreatic cancer and shortness of breath demonstrate a filling defect at a branching point within the left lower lobe pulmonary artery, with extension into the segmental arterial branches (*arrow*). Three-dimensional (3-D) volume-rendered displays (**b, c**) help demonstrate the full extent of this embolus (*arrows*)

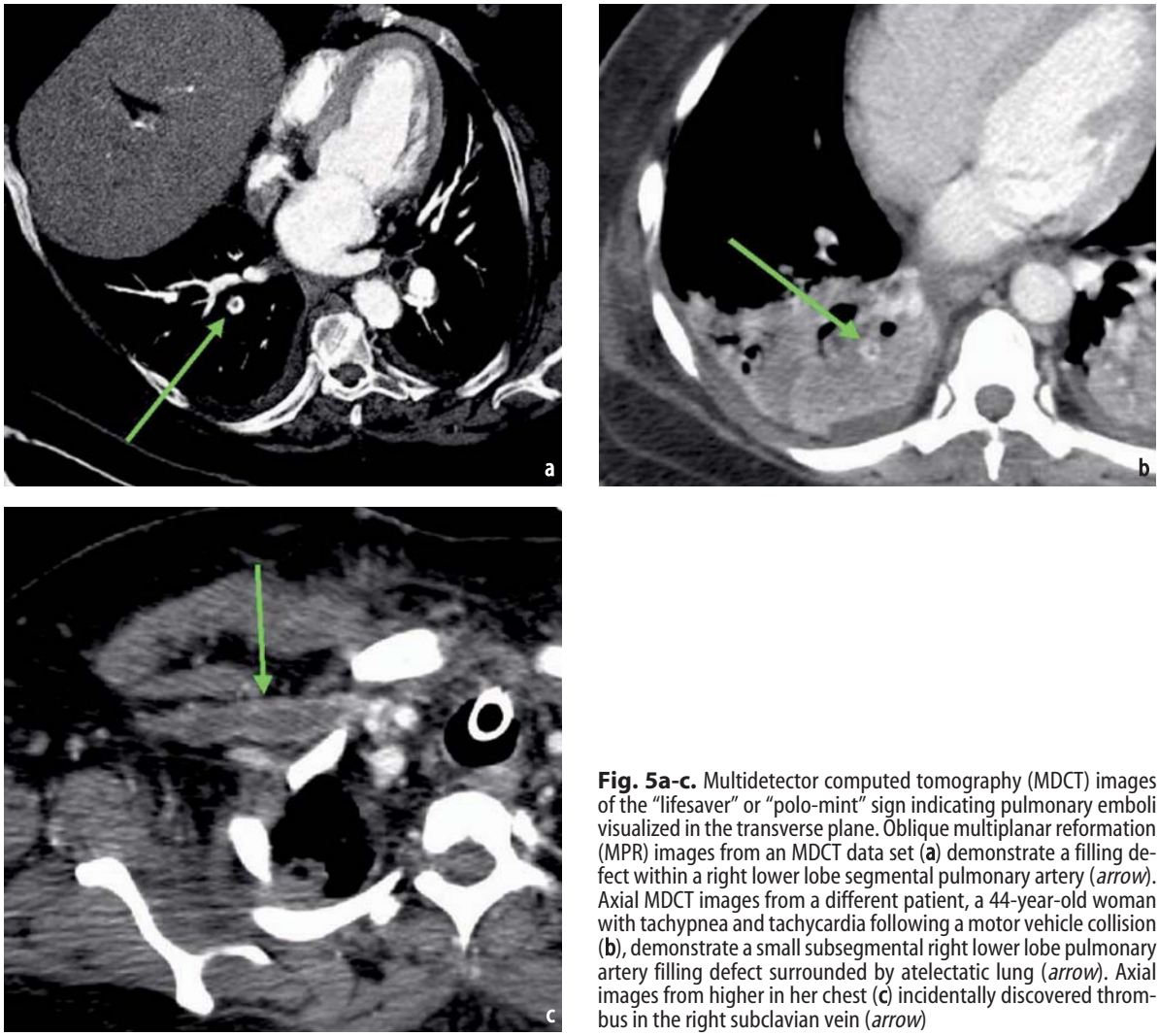

Fig. 5a-c. Multidetector computed tomography (MDCT) images of the "lifesaver" or "polo-mint" sign indicating pulmonary emboli visualized in the transverse plane. Oblique multiplanar reformation (MPR) images from an MDCT data set (**a**) demonstrate a filling defect within a right lower lobe segmental pulmonary artery (*arrow*). Axial MDCT images from a different patient, a 44-year-old woman with tachypnea and tachycardia following a motor vehicle collision (**b**), demonstrate a small subsegmental right lower lobe pulmonary artery filling defect surrounded by atelectatic lung (*arrow*). Axial images from higher in her chest (**c**) incidentally discovered thrombus in the right subclavian vein (*arrow*)

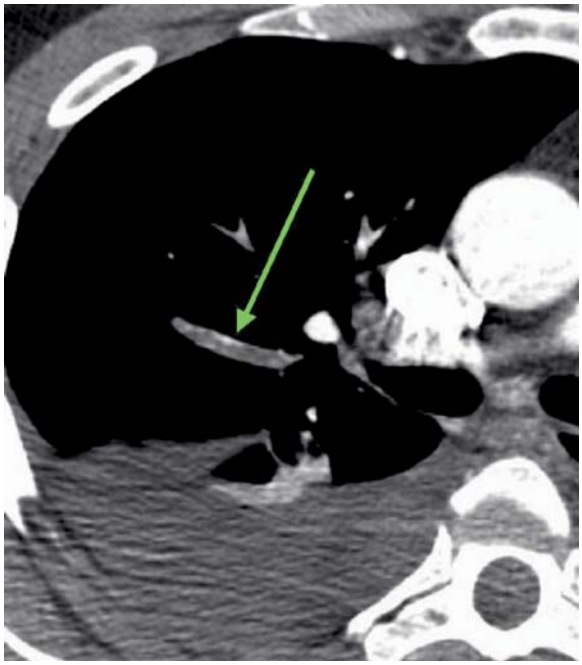

Fig. 6. Multidetector computed tomography (MDCT) images from CT pulmonary angiography in the axial plane demonstrate thrombus tracking longitudinally through a right middle lobe pulmonary artery feeding the lateral segment (*arrow*) with a characteristic "railway-track" appearance

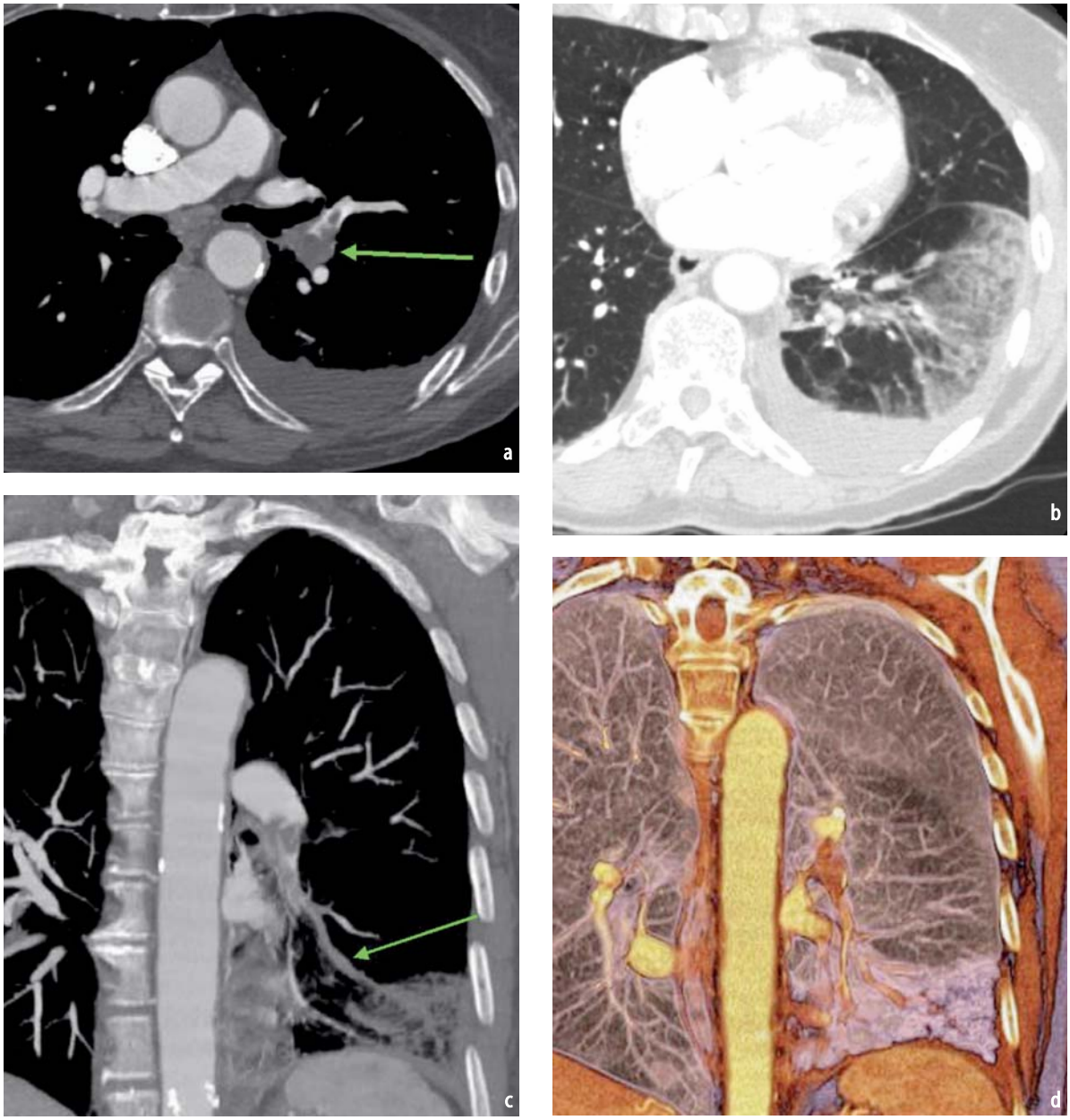

Fig. 7a-d. An 80-year-old woman presented with chest pain on the left with deep inspiration. Single-axial contrast-enhanced image (**a**) demonstrates a large embolus within the left main pulmonary artery extending into the left lower lobe pulmonary artery (*arrow*). Axial slice examined using lung windows (**b**) demonstrates a wedge-shaped region of ground-glass opacity in the periphery of the left lower lobe consistent with hemorrhage. Coronal multiplanar reconstruction (MPR) image (**c**) shows thrombus extending into the area of hemorrhage (*arrow*). Coronal three-dimensional (3-D) volume rendering (**d**) again demonstrates the large embolus and area of hemorrhage

Prognostic Value of CT in PE Patients

In addition to diagnosing emboli and other potential etiologies of dyspnea and chest pain, CT may provide some insight into the prognosis of patients with PE. There are cardiac findings on CT that may portend a worse clinical prognosis or warrant more emergent care in an intensive care unit and possible catheter intervention, thrombolysis, or surgical embolectomy, in addition to anticoagulation. Poor prognostic factors relate to the degree of right ventricular dysfunction and include the degree of right ventricular enlargement (Fig. 10), pulmonary artery thrombus load, enlargement of the main pulmonary artery, reflux of contrast into the hepatic veins (Fig. 11), and bowing of the ventricular septum toward the left ventricle.

Patients with a right ventricular diameter to

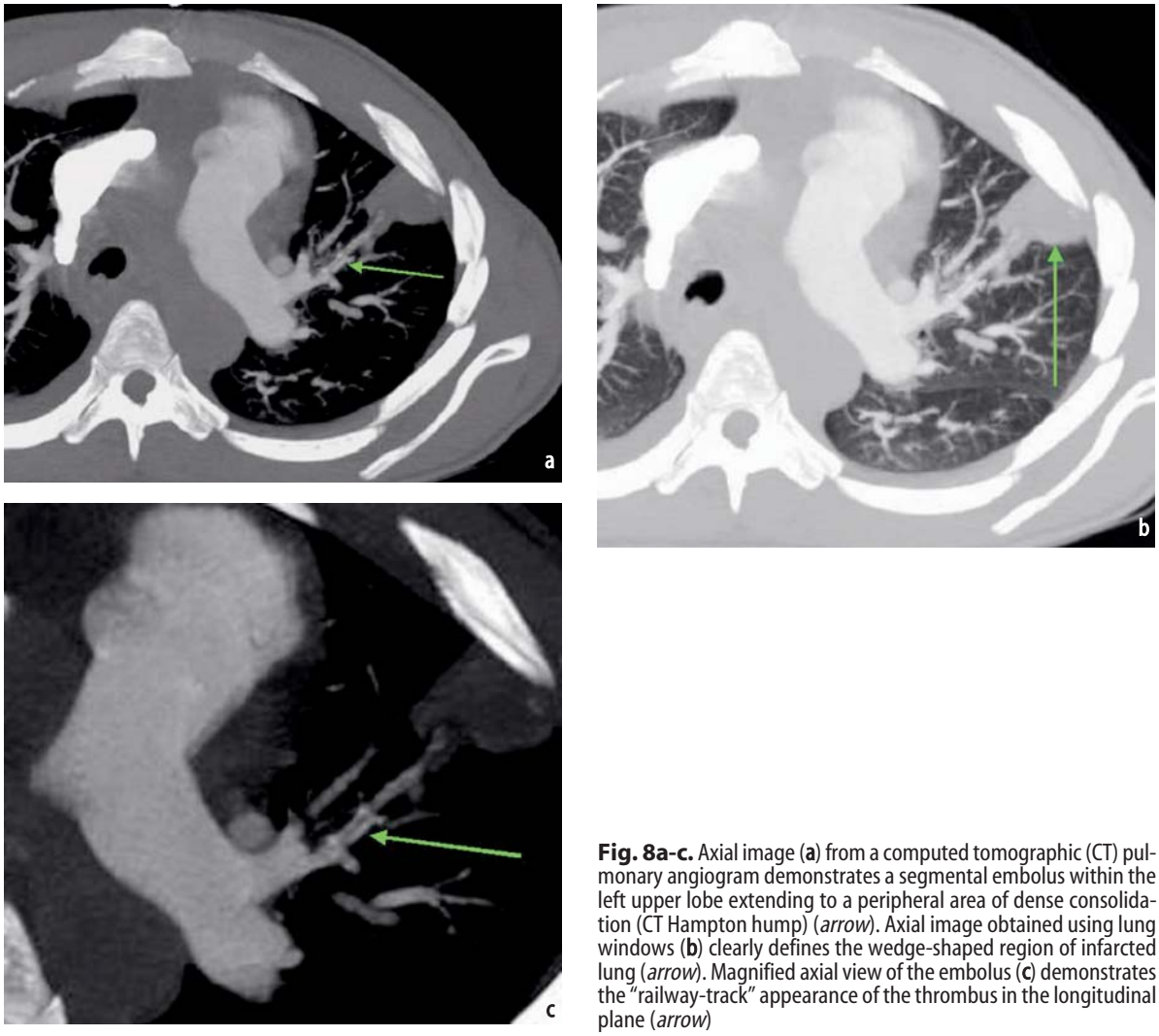

Fig. 8a-c. Axial image (**a**) from a computed tomographic (CT) pulmonary angiogram demonstrates a segmental embolus within the left upper lobe extending to a peripheral area of dense consolidation (CT Hampton hump) (*arrow*). Axial image obtained using lung windows (**b**) clearly defines the wedge-shaped region of infarcted lung (*arrow*). Magnified axial view of the embolus (**c**) demonstrates the "railway-track" appearance of the thrombus in the longitudinal plane (*arrow*)

left ventricular diameter (RVD/LVD) ratio of greater than 0.9 have a significant increase in mortality and a much greater likelihood of major complications [45–47]. One study showed a positive predictive value for PE-related mortality of 10.1% within the first 3 months after the diagnosis of PE with right ventricular enlargement (RVD/LVD ratio greater than 1.0). Perhaps more significantly, in those patients with a RVD/LVD ratio less than 1.0, there was a negative predictive value of 100% for an uneventful course [48]. Therefore, those patients without right ventricular enlargement are less unlikely to have an adverse outcome and are more likely to survive. Therefore, signs of right heart strain should be mentioned in the report and discussed with the referring physician, as they represent important prognostic factors that could assist in treatment planning and patient placement.

Studies have also shown a relationship between the percentage of pulmonary vascular bed obstruction and 3-month mortality. A scoring system based upon the number and degree of vascular obstructions was utilized. The highest possible score of 40 indicates complete obstruction of the pulmonary trunk [49]. Patients with a degree of vascular obstruction of greater than 40% have an 11% increased risk of dying from PE within the first 3 months. The negative predictive value in patients with a less than 40% degree of obstruction was 99%; indicating a very low rate of PE-related mortality [48, 50].

PE Protocol Using MDCT

Protocols employed for the detection of PE have evolved with rapid advances in CT technology. Current MDCT scanners are capable of providing

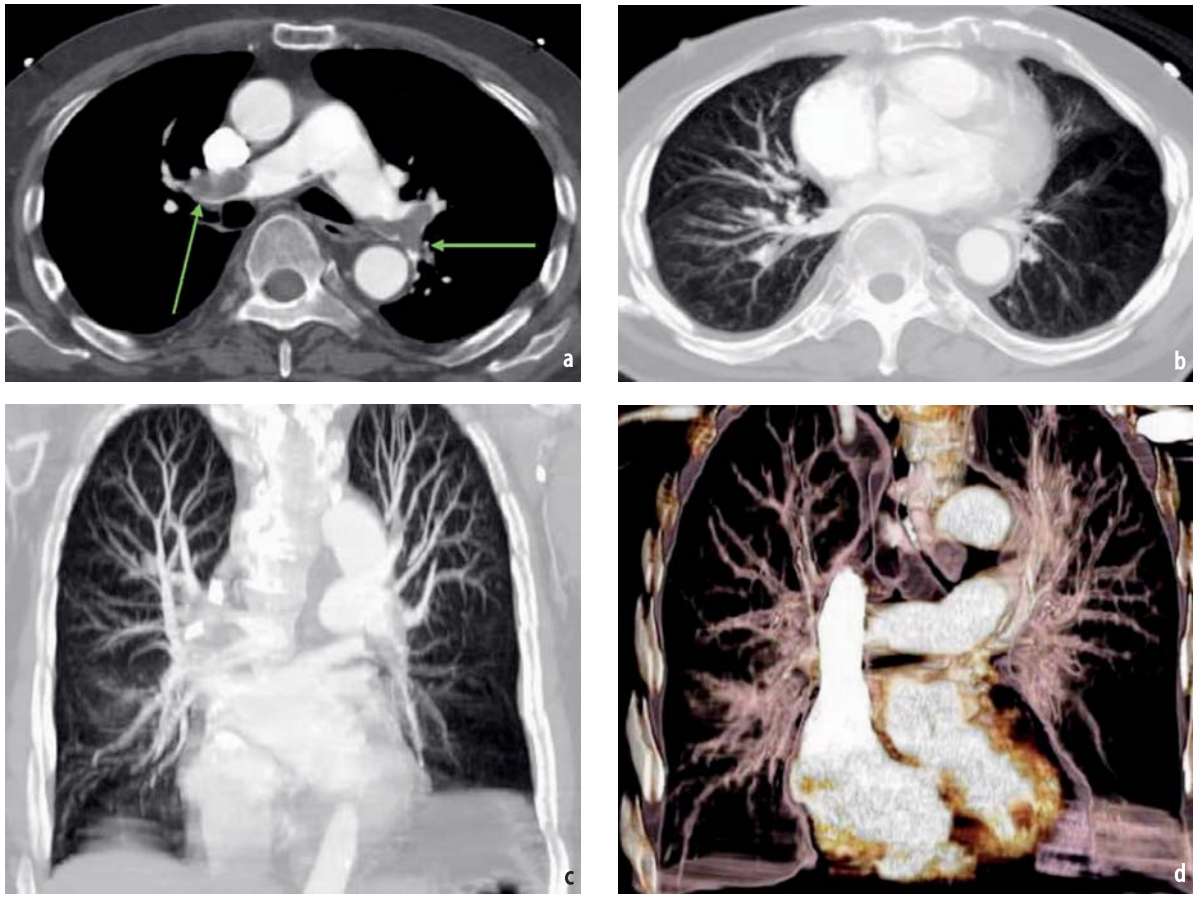

Fig. 9a-d. Axial image from a multidetector computed tomography (MDCT) pulmonary angiogram (**a**) demonstrates bilateral pulmonary emboli in a patient with acute shortness of breath and right lower extremity swelling (*arrows*). Axial image through the lower lobes using lung windows (**b**) demonstrates oligemia in the left lower lobe (CT Westermark sign). Coronal multiplanar reconstruction (MPR) image (**c**) again demonstrates the asymmetric hypovascularity in the left lower lobe. Three-dimensional (3-D) volume rendering in the coronal plane (**d**) more clearly defines the region of oligemia

image resolution of less than 1 mm. Patient respiratory motion artifacts have decreased dramatically over the last few years as acquisition of the entire thorax can be obtained in under 10 s using a 16-slice scanner and in less than 5 s with 64-slice units.

The quality of enhancement of the pulmonary arteries relies on several parameters: the amount and concentration of contrast agent used, the injection rate, and the delay between injection and scanning. To ensure adequate opacification of the pulmonary arteries, images are obtained 20 s following intravenous administration or, preferably, by using bolus tracking software to determine peak contrast delivery to the pulmonary arteries (Table 1).

Scan delay is obtained by injecting 15 ml of contrast material and placing a region of interest over the main pulmonary artery. Using a high concentration contrast agent, such as Isovue-370, and a rapid flow rate of up to 4 ml/s ensures ideal vascular opacification. Injection of contrast media is typically via an 18- or 20-gauge peripheral intravenous line, preferably through the antecubital vein. A saline chaser may be used to decrease the amount of beam-hardening artifact caused by dense opacification of the superior vena cava and to decrease the amount of iodinated contrast needed to adequately opacify the pulmonary arteries [51–53]. While shorter scan times decrease respiratory motion and associated artifacts, timing the delivery of contrast becomes very critical with 16- and 64-slice protocols (Table 1).

In patients who are physically larger than average, 2.0–2.5 mm acquisitions can be used to decrease quantum mottle [43]. ECG gating has been recently implemented in some institutions to eliminate cardiac pulsation artifacts seen in small ves-

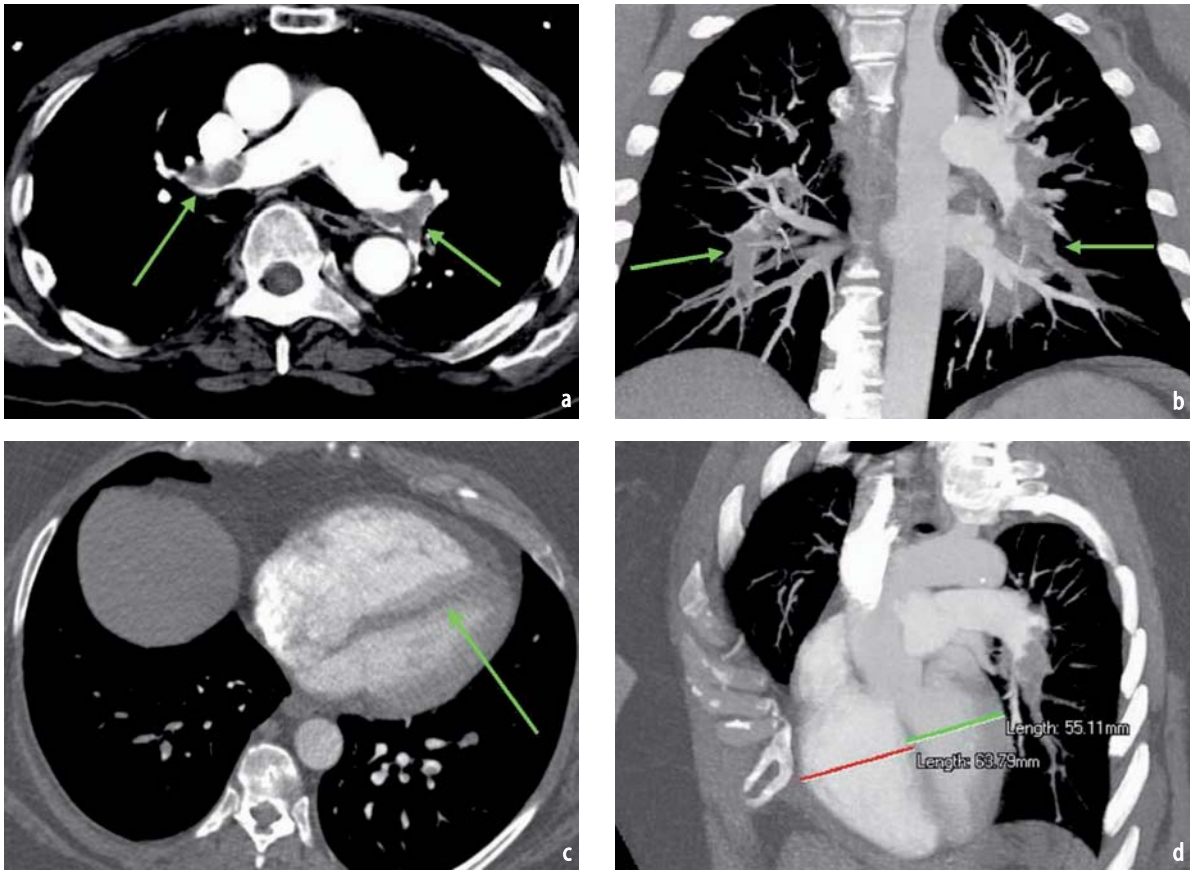

Fig. 10a-d. Computed tomographic (CT) pulmonary angiogram performed in a 49-year-old woman with chest pain and shortness of breath. Axial image through the pulmonary arteries (**a**) demonstrates large emboli within the left and right pulmonary arteries (*arrows*). Coronal multiplanar reconstruction (MPR) image (**b**) more clearly demonstrates the extent of the emboli (*arrows*). Axial image through the ventricular septum (**c**) reveals straightening of the septum and dilation of the right ventricle (*arrow*). Further evaluation with oblique MPR (**d**) clearly shows a right ventricular diameter (*red line*) that is larger than the left ventricular (*green line*) diameter (RVD/LVD ratio >1) consistent with right ventricular dysfunction

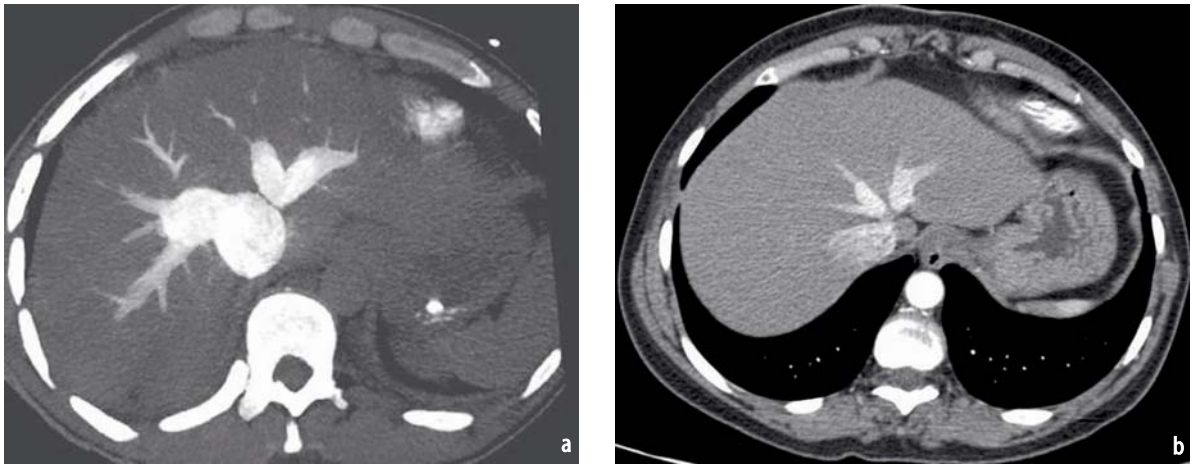

Fig. 11a, b. Axial images (**a**, **b**) obtained during multidetector computed tomography (MDCT) pulmonary angiography in two different patients show reflux of intravenous contrast into the hepatic veins, which is a sign of right ventricular dysfunction. The first image (**a**) also demonstrates distention of the hepatic veins. Both patients had large pulmonary emboli

Table 1. Computed tomography (CT) protocols: CT pulmonary angiography

Scanner type	4 slice	16 slice	64 slice
Collimation		16 × 0.75	64 × 0.6
Reconstruction (mm)	1.25	1.00	0.75
Rotation time (s)	0.8	0.5	0.33
Contrast volume (370 mgI/mL)	100 ml	100 ml	75–100 ml
Saline flush		50 ml	50 ml

sels adjacent to the heart; however, this technique requires a longer breath hold and increased radiation exposure. When viewing the pulmonary arterial system, window and level settings should be placed around 700 and 1,000 Hounsfield units (HU), respectively [43, 54].

Currently employed MDCT yields very large numbers of axial images – up to 1,000 with some newer systems. This can result in difficulties for the interpreting radiologist due to the sheer number of images to review. Two potential solutions include display tools and computer-aided diagnosis (CAD), which allow for rapid production of maximum intensity projection (MIP) images, multiplanar reconstructions (MPR), and three-dimensional (3-D) reformations. These reformations and reconstructions of the source images allow improved visualization of distal subsegmental pulmonary arterial branches with reconstruction of fewer overall images, without sacrificing PE detection sensitivity. CAD tools are under development and may be used as a second reader, potentially reducing study reading times. Preliminary experience in a small study population showed CAD tools can detect segmental emboli but are currently inaccurate for subsegmental emboli [55].

Disadvantages to MDCT

Approximately 3% of the CT scans completed for PE at our institution are inadequate for accurate interpretation [56]. Most problems relate to technical factors, including poor bolus timing and poor venous access. Correctly applied bolus tracking with density measurements over the pulmonary artery provides scan-precise delay times and optimal enhancement of the pulmonary arteries. Beam-hardening artifacts from dense contrast bolus within the superior vena cava may obscure small emboli in adjacent vessels (Fig. 12), particularly in the right main and right upper lobe pulmonary arteries [43]. Saline bolus chasing following initial contrast injection with a dual-head injector can eliminate these artifacts completely. Abrupt loss of pulmonary artery opacification caused by the mixing of unopacified blood from the inferior vena cava may occur. This pulmonary artery flow artifact, also known as a "stripe sign," occurs during inspiration and results in loss of the contrast column in the pulmonary arteries; thus mimicking emboli [57, 58].

Patient factors that may hinder PE interpretation most often involve a large patient body habitus, leading to increased quantum mottle or an inability to breath hold for the desired length of time, resulting in motion artifact. Additional diagnostic pitfalls include partial volume averaging from hilar lymph nodes and mucous-filled bronchi. By utilizing a combination of workstation analysis, MIP, and MPR, both lymph nodes and mucous-filled bronchi can be distinguished from adjacent pulmonary arteries [59].

Radiation dose considerations with CT require careful evaluation when developing protocols. During a typical CT pulmonary angiogram, the effective patient dose ranges from 4-8 mSv, with an absorbed breast dose of 21 mGy [60]. As a comparison, the absorbed breast dose during a screening mammogram is only 2.5 mGy [60]. However, the risk-to-benefit ratio of using CT for diagnosing PE typically weighs heavily in favor of performing the study. CT pulmonary angiography using a single-slice scanner utilizes a radiation dose five times less than that of conventional angiography [61]. Performing CT examinations in young or pregnant women requires special considerations. In a young woman with a negative chest radiograph and low-to-moderate clinical suspicion, a V/Q scan might be considered as a more appropriate option. However, many patients undergo a subsequent CT study, so additional radiation burden to the female breast should be carefully evaluated. In pregnant patients with suspected PE, CT is recommended over V/Q scintigraphy, as the absorbed radiation dose to the fetus is 1–2 mGy for V/Q scans versus 0.1-0.2 mGy for CT [62, 63].

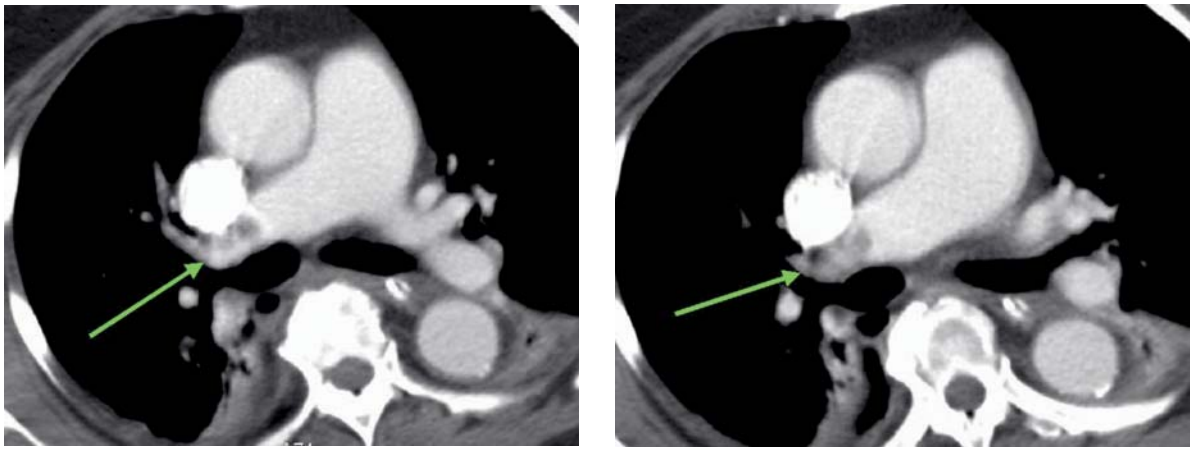

Fig. 12a, b. A 76-year-old woman who was postoperatively day 1 from a bilateral salpingooophorectomy presented with decreased breath sounds in the right lung base, decreased oxygen saturation, and increased A-a gradient. Subsequent axial images from a contrast-enhanced multidetector computed tomography (MDCT) study (**a, b**) demonstrate beam-hardening artifact almost completely obscuring a large thrombus within the right main pulmonary artery (*arrows*). A saline chaser following injection of the iodinated contrast would have eliminated this artifact

Role of D-Dimer

D-dimer enzyme-linked immunosorbent assays (ELISA) play an important role in the workup for possible PE. D-dimer is a highly sensitive test (97%) with a negative predictive value of 99.6% [4]. This inexpensive measurement is an effective screening test in the outpatient setting for suspected PE. As a result, further diagnostic tests would be unnecessary in patients with a negative D-dimer assay, as there would be a very low likelihood of PE [64, 65]. Taking this one step further, Perrier et al. [28] showed that patients have a very low likelihood of having any adverse affects related to PE when there is a negative CT angiogram and a negative D-dimer assay. Therefore, these patients are not only unlikely to have a PE, but they are also unlikely to suffer any adverse events secondary to venous thromboembolism within 3 months of the negative diagnostic tests. Unfortunately, the D-dimer assay is highly nonspecific and is of limited value within the inpatient setting. Other etiologies resulting in elevated D-dimer assays include cancer, myocardial infarction, pneumonia, sepsis, and pregnancy.

Future of MDCT

With continued technological improvements, MDCT pulmonary angiography will continue to be the test of choice for the diagnosis of PE. It is likely that these advances will center not only on hardware but also on the software used to reformat the large amount of acquired data during the CT examination. With slice thickness under 1.00 mm, there may be up to 1,000 axial images for the radiologist to evaluate. Unfortunately, small pulmonary emboli may be "overlooked" by having to individually examine each acquired image. In retrospect, these "perceptual errors" may be readily detectable: 60% of missed diagnoses occur because the embolus was simply not seen on first examination [66, 67]. CAD for PE has shown potential for limiting these perceptual errors [68, 69].

Advancements in the software used to create 2-D and 3-D reformations of the axial CT data will continue to improve our ability to detect emboli in obliquely oriented pulmonary arteries (Fig. 13) [70]. One promising technique involves performing "paddle wheel" reformations of the pulmonary arteries. A horizontal axis centered at the lung hila is used as a pivot point to image the pulmonary arteries. This type of multiplanar volume reformation helps prevent the "slicing" of pulmonary arteries into small fragments that are seen on coronal and sagittal reformations. Presumably, this will not only improve visualization of the pulmonary arterial tree but also decrease the overall number of images for the radiologist to review to accurately diagnose PE [71, 72].

Studies are also underway to assess the possibility of using a single, contrast-enhanced, ECG-gated CT scan to assess patients with chest pain for coronary artery disease, pulmonary disease, and aortic disease [73]. Results of PIOPED II, which prospectively compared V/Q scanning, Doppler sonography for DVT, digital subtraction pulmonary angiography, and contrast venography with MDCT for the detection of venous thromboembolism [41], may provide practice guidelines.

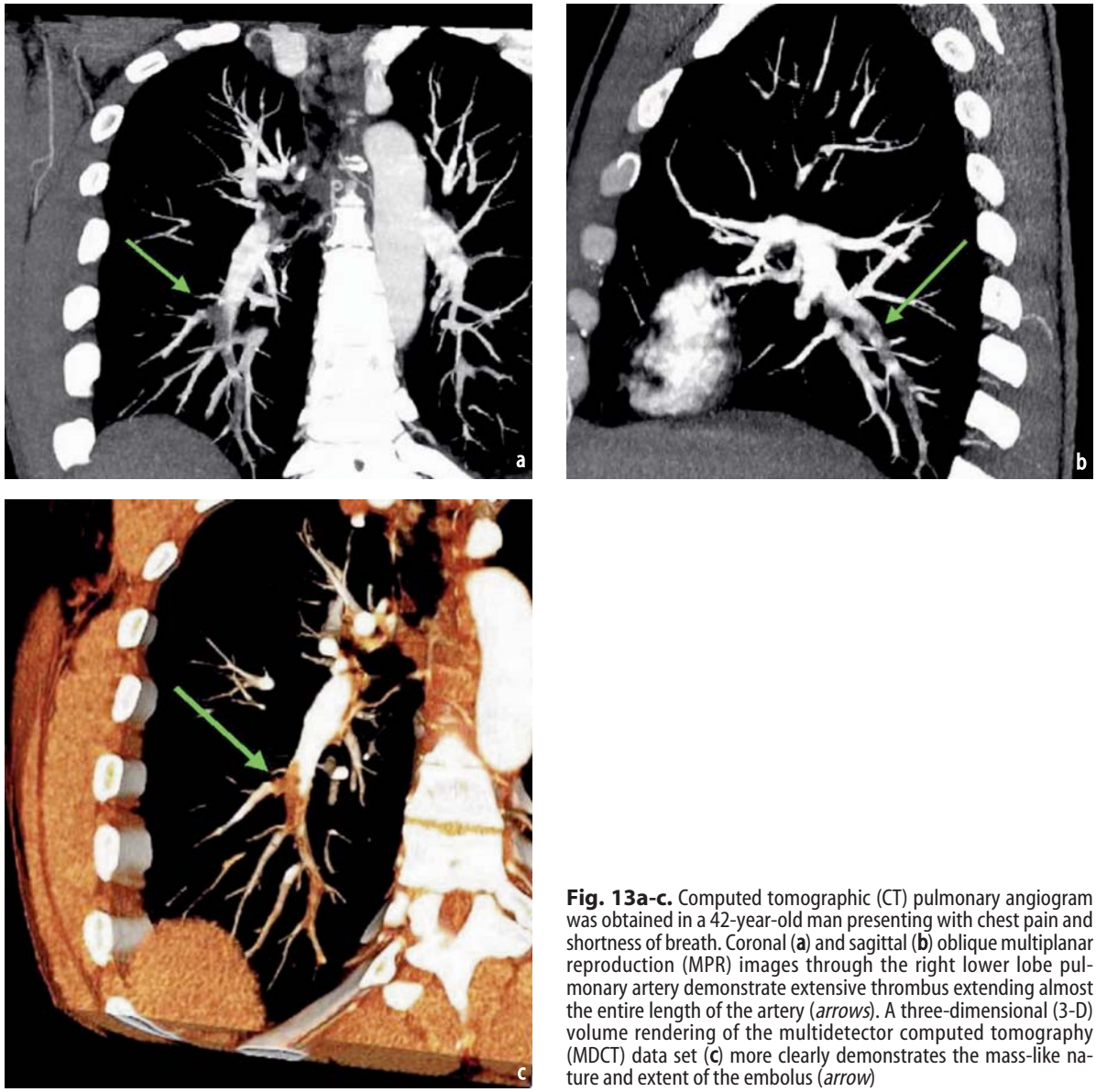

Fig. 13a-c. Computed tomographic (CT) pulmonary angiogram was obtained in a 42-year-old man presenting with chest pain and shortness of breath. Coronal (**a**) and sagittal (**b**) oblique multiplanar reproduction (MPR) images through the right lower lobe pulmonary artery demonstrate extensive thrombus extending almost the entire length of the artery (*arrows*). A three-dimensional (3-D) volume rendering of the multidetector computed tomography (MDCT) data set (**c**) more clearly demonstrates the mass-like nature and extent of the embolus (*arrow*)

Conclusion

CT pulmonary angiography has become the imaging modality of choice for the detection of acute PE. MDCT has proven sensitivity and specificity for detecting small pulmonary emboli in distal subsegmental pulmonary arteries with high interobserver agreement and cost effectiveness. Additionally, CT allows for the detection of other etiologies that may or may not be contributing to the patient's clinical presentation. When combined with CT venography, MDCT now provides a standalone test for excluding venous thromboembolism. High-risk patients with right ventricular dysfunction are also readily identifiable with CT pulmonary angiography, allowing for more appropriate management. Furthermore, continued improvements in postacquisition reformations and CAD will continue to enhance the ability to detect pulmonary emboli with an accuracy far exceeding that of other modalities.

References

1. Carson JL, Kelley MA, Duff A et al (1992) The clinical course of pulmonary embolism. N Engl J Med 326(19):1240–1245
2. Goldhaber SZ, Elliott CG (2003) Acute pulmonary embolism: part I: epidemiology, pathophysiology, and diagnosis. Circulation 108(22):2726–2729
3. Daniel KR, Courtney DM, Kline JA (2001) Assessment of cardiac stress from massive pulmonary embolism with 12-lead ECG. Chest 120:474–481
4. Dunn KL, Wolf JP, Dorfman DM et al (2002) Normal D-dimer levels in emergency department pa-

tients suspected of acute pulmonary embolism. J Am Coll Cardiol 40:1475–1478
5. Elliott CG, Goldhaber SZ, Visani L et al (2000) Chest radiographs in acute pulmonary embolism. Results from the international cooperative pulmonary embolism registry. Chest 118:33–38
6. Ferrari E, Imbert A, Chevalier T et al (1997) The ECG in pulmonary embolism: predictive value of negative T waves in precordial leads: 80 case reports. Chest 111:537–543
7. Kucher N, Walpoth N, Wustmann K et al (2003) QR in V1: an ECG sign associated with right ventricular strain and adverse clinical outcome in pulmonary embolism. Eur Heart J 24:1113–1119
8. Stein PD, Goldhaber SZ, Henry JW (1995) Alveolar-arterial oxygen gradient in the assessment of acute pulmonary embolism. Chest 107:139–143
9. Stein PD, Goldhaber SZ, Henry JW et al (1996) Arterial blood gas analysis in the assessment of suspected acute pulmonary embolism. Chest 109:78–81
10. Prologo JD, Glauser J (2002) Variable diagnostic approach to suspected pulmonary embolism in the ED of a major academic tertiary care center. Am J Emerg Med 20:5–9
11. Prologo JD, Gilkeson RC, Diaz M et al (2004) CT Pulmonary angiography: A comparative analysis of the utilization patterns in emergency department and hospitalized patients between 1998 and 2003. AJR Am J Roentgenol 183:1093–1096
12. Stein PD, Kayali F, Olson RE (2004) Trends in the use of diagnostic imaging in patients hospitalized with acute pulmonary embolism. Am J Cardiol 93:1316–1317
13. Kim KI, Muller NL, Mayo JR (1999) Clinically suspected pulmonary embolism: utility of spiral CT. Radiology 210:693–697
14. Kavanagh EC, O'Hare A, Hargaden G (2004) Risk of pulmonary embolism after negative MDCT pulmonary angiography findings. AJR Am J Roentgenol 182:499–504
15. Blachere H, Latrabe V, Montaudon M et al (2000) Pulmonary embolism revealed on helical CT angiography: comparison with ventilation-perfusion radionuclide lung scanning. AJR Am J Roentgenol 174:1041–1047
16. Bourriot K, Couffinhal T, Bernard V et al (2003) Clinical outcome after a negative spiral CT pulmonary angiographic finding in an inpatient setting from cardiology and pneumology wards. Chest 123:359–365
17. Garg K, Sieler H, Welsh CH et al (1999) Clinical validity of helical CT being interpreted as negative for pulmonary embolism: implications for patient treatment. AJR Am J Roentgenol 172:1627–1631
18. Goodman LR, Lipchik RJ, Kuzo RS et al (2000) Subsequent pulmonary embolism: risk after a negative helical CT pulmonary angiogram – prospective comparison with scintigraphy. Radiology 215: 535–542
19. Lomis NN, Yoon HC, Moran AG et al (1999) Clinical outcomes of patients after a negative spiral CT pulmonary arteriogram in the evaluation of acute pulmonary embolism. J Vasc Interv Radiol 10:707–712
20. Ost D, Rozenshtein A, Saffran L et al (2001) The negative predictive value of spiral computed tomography for the diagnosis of pulmonary embolism in patients with nondiagnostic ventilation-perfusion scans. Am J Med 110:16–21
21. Tillie-Leblond I, Mastora I, Radenne F et al (2002) Risk of pulmonary embolism after a negative spiral CT angiogram in patients with pulmonary disease: 1-year clinical follow-up study. Radiology 223: 461–467
22. Gottsater A, Berg A, Certergard J et al (2001) Clinically suspected pulmonary embolism: is it safe to withhold anticoagulation after a negative spiral CT? Eur Radiol 11:65–72
23. Krestan CR, Klein N, Fleischmann et al (2004) Value of negative spiral CT angiography in patients with suspected acute PE: analysis of PE occurrence and outcome. Eur Radiol 14:93–98
24. Musset D, Parent F, Meyer G et al (2002) Diagnostic strategy for patients with suspected pulmonary embolism: a prospective multicentre outcome study. Lancet 360:1914–1920
25. Nilsson T, Olausson A, Johnsson H et al (2002) Negative spiral CT in acute pulmonary embolism. Acta Radiol 43:486–491
26. Qanadli SC, Hajjam ME, Mesurolle B et al (2000) Pulmonary embolism detection: prospective evaluation of dual-section helical CT versus selective pulmonary arteriography in 157 patients. Radiology 217:447–455
27. Swensen SJ, Sheedy PF II, Ryu JH et al (2002) Outcomes after withholding anticoagulation from patients with suspected acute pulmonary embolism and negative computed tomographic findings: a cohort study. Mayo Clin Proc 77:130–138
28. Perrier A, Pierre-Marie R, Sanchez O et al (2005) Multidetector-row computed tomography in suspected pulmonary embolism. N Engl J Med 352:1760–1768
29. Henry JW, Stein PD, Gottschalk A et al (1996) Scintigraphic lung scans and clinical assessment in critically ill patients with suspected acute pulmonary embolism. Chest 109:462–466
30. PIOPED Investigators (1990) Value of the ventilation/perfusion scan in acute pulmonary embolism JAMA 95:498–502
31. Quiroz R, Kucher N, Zou KH et al (2005) Clinical validity of a negative computed tomography scan in patients with suspected pulmonary embolism – a systematic review. JAMA 293:2012–2017
32. van Beek EJ, Reekers JA, Batcherlor DA et al (1995) Feasibility, safety and clinical utility of angiography in patients with normal pulmonary angiograms. Chest 107:1375–1378
33. Ghaye B, Szapiro D, Mastora I et al (2001) Peripheral pulmonary arteries: how far in the lung does multi-detector row spiral CT allow analysis? Radiology 219:629–636
34. Patel S, Kazerooni EA, Cascade PN (2003) Pulmonary embolism: optimization of small pulmonary artery visualization at multi-detector row CT. Radiology 227:455–460
35. Schoepf UJ, Holzknecht N, Helmberger TK et al (2002) Subsegmental pulmonary emboli: improved detection with thin-collimation multi-detector row spiral CT. Radiology 222:483–490
36. Diffin DC, Leyendecker JR, Johnson SP et al (1998) Effect of anatomic distribution of pulmonary emboli on interobserver agreement in the interpretation of pulmonary angiography. AJR Am J

Roentgenol 171:1085–1089
37. Stein PD, Henry JW, Gottschalk A (1999) Reassessment of pulmonary angiography for the diagnosis of pulmonary embolism: relation of interpreter agreement to the order of the involved pulmonary arterial branch. Radiology 210:689–691
38. Washington L (2005) Venous thromboembolism: epidemiologic, clinical, and imaging perspectives. Cardiopulmonary imaging, categorical course syllabus. American Roentgen Ray Society 41–51
39. Cosmic MS, Goodman LR, Lipchik RJ et al (2002) Detection of deep venous thrombosis with combined helical CT scan of the chest and CT venography in unselected cases of suspected pulmonary embolism. Am J Respir Crit Care Med 165:A329
40. Ghaye B, Remy J, Remy-Jardin M et al (2002) Nontraumatic thoracic emergencies: CT diagnosis of acute pulmonary embolism-the first 10 years. Eur Radiol 12:1886–1905
41. Gottschalk A, Stein PD, Goodman LR et al (2002) Overview of prospective investigation of pulmonary embolism diagnosis II. Semin Nucl Med 32:173–182
42. Washington L, Goodman LR, Gonyo MB (2002) CT for thromboembolic disease. Radiol Clin North Am 40:751–771
43. Wittram C, Maher MM, Yoo AJ et al (2004) CT angiography of pulmonary embolism: diagnostic criteria and causes of misdiagnosis. Radiographics 24:1219–1238
44. Shah AA, Davis SD, Gamsu G et al (1999) Parenchymal and pleural findings in patients with and patients without acute pulmonary embolism detected at spiral CT. Radiology 211:147–153
45. Quiroz R, Kucher N, Schoepf UJ et al (2004) Right ventricular enlargement on chest computed tomography: prognostic role in acute pulmonary embolism, Circulation 109:2401–2404
46. Reid JH, Murchison JT (1998) Acute right ventricular dilation: a new helical CT sign of massive pulmonary embolism. Clin Radiol 53:694–698
47. Schoepf UJ, Kucher N, Kipfmueller F et al (2004) Right ventricular enlargement on chest computed tomography: a predictor of early death in acute pulmonary embolism. Circulation 110:3276–3280
48. Van der Meer RW, Pattynama PM, van Strijen MJ et al (2005) Right ventricular dysfunction and pulmonary obstruction index at helical CT: prediction of clinical outcome during 3-month follow-up in patients with acute pulmonary embolism. Radiology 235:798–803
49. Qanadli SD, El Hajjam M, Vieillard-Baron A et al (2001) New CT index to quantify arterial obstruction in pulmonary embolism: comparison with angiographic index and echocardiography. AJR Am J Roentenol 176(6):1415–1420
50. Wu AS, Pezzullo JA, Cronan JJ et al (2004) CT pulmonary angiography: quantification of pulmonary embolus as a predictor of patient outcome – initial experience. Radiology 230:831–835
51. Cademartiri F, Mollet N, van der Lugt A et al (2004) Non-invasive 16–row multislice CT coronary angiography: usefulness of saline chaser. Eur Radiol 14:178–183
52. Dorio PJ, Lee FT, Henseler KP et al (2003) Using a saline chaser to decrease contrast media in abdominal CT. AJR Am J Roentgenol 180:929–934
53. Haage P, Schmitz-Rode T, Hubner D et al (2000) Reduction of contrast material dose and artifacts by a saline flush using a double power injector in helical CT of the thorax. AJR Am J Roentgenol 174: 1049–1053
54. Storto ML, Di Credico A, Guido F et al (2005) Incidental detection of pulmonary emboli on routine MDCT of the chest AJR Am J Roentgenol 184: 264–267
55. Schoepf UJ, Schneider AC, Das M et al (2005) Pulmonary embolism: computer aided detection at multi-detector row spiral CT. Radiology (*in press*)
56. Schoepf UJ, Savino G, Lake DR et al (2005) The age of CT pulmonary angiography. J Thorac Imaging 20(4):273-279
57. Gosselin MV, Rassner UA, Thieszen SL et al (2004) Contrast dynamics during CT pulmonary angiogram: analysis of an inspiration associated artifact. J Thorac Imaging 19:1–7
58. Yoo AJ, Wittram C (2003) CTPA pulmonary artery flow artifact: pitfall in the diagnosis of pulmonary embolism Radiology 352(P):233
59. Gruden JF (2005) Pulmonary embolism: MDCT technique and interpretative pitfalls. Cardiopulmonary imaging, categorical course syllabus. American Roentgen Ray Society 53–60
60. Wiest PW, Locken JA, Heintz PH et al (2002) CT scanning: a major source of radiation exposure. Semin Ultrasound CT MR 23(5):402–410
61. Resten A, Mausoleo F, Valero M, Musset D (2003) Comparison of doses for pulmonary embolism detection with helical CT and pulmonary angiography. Eur Radiol 13:1515–1521
62. Huda W (2005) When a pregnant patient has a suspected pulmonary embolism, what are the typical embryo doses from a chest CT and a ventilation/perfusion study? Pediatr Radiol 25:25
63. Winer-Muram HT, Boone JM, Brown HL et al (2002) Pulmonary embolism in pregnant patients: fetal radiation dose with helical CT. Radiology 224(2):487–492
64. Abcarian PW, Sweet JD, Watabe JT et al (2004) Role of a quantitative D-dimer assay in determining the need for CT angiography of acute pulmonary embolism. AJR Am J Roentgenol 182:1377–1381
65. Kline JA, Wells PS (2003) Methodology for a rapid protocol to rule out pulmonary embolism in the emergency department. Ann Emerg Med 42: 266–275
66. Berlin L (1996) Malpractice issues in radiology. Perceptual errors. AJR Am J Roentgenol 167:587–590
67. Renfrew DL, Franken EA Jr, Berbaum KS et al (1992) Error in radiology: classification and lessons in 182 cases presented at a problem case conference. Radiology 183:145–150
68. Peldschus K, Herzog P, Wood SA et al (2005) Computer-aided diagnosis as a second reader: Spectrum of findings in computed tomography studies of the chest interpreted as normal. Chest 128:1517–1523
69. Wittram C, Meehan MJ, Halpern EF et al (2004) Trends in thoracic radiology over a decade at a large academic medical center. J Thorac Imaging 19: 164–170
70. Remy-Jardin M, Remy J, Cauvain O et al (1995): Diagnosis of central pulmonary embolism with helical CT: role of two-dimensional multiplanar reformations. AJR Am J Roentgenol 165:1131–1138

71. Chiang EE, Boiselle PM, Raptopoulos V et al (2003) Detection of pulmonary embolism: comparison of paddlewheel and coronal CT reformations – initial experience. Radiology 228:577–582
72. Simon M, Chiang EE, Boiselle PM (2001) Paddlewheel multislice helical CT display of pulmonary vessels and other lung structures. Radiol Clin North Am 41:617–626
73. Schoepf UJ, Becker CR, Ohnesorge BM et al (2004) CT of coronary artery disease. Radiology 232:18–37